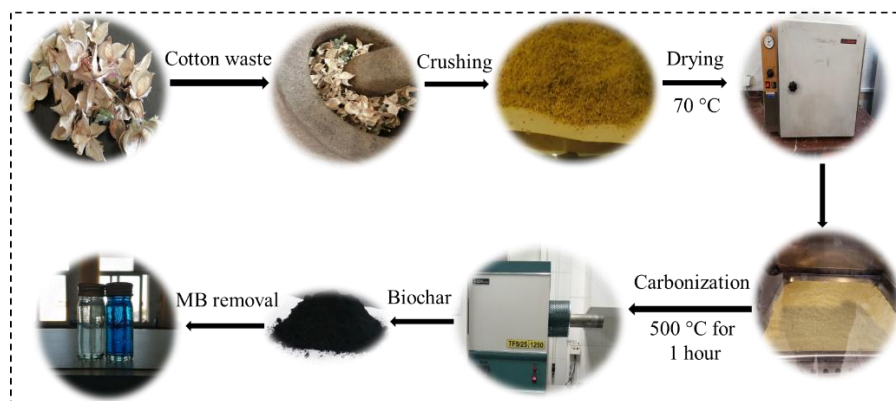


Adsorption potential of biochar derived from cotton waste for efficient removal of methylene blue from aqueous solutions

Samaneh Salmani^{id}, Hassan Rezaei^{*id}, Hajar Abyar^{id}

Department of Environmental Sciences, Faculty of Fisheries and Environmental Sciences, Gorgan University of Agricultural Sciences and Natural Resources, Gorgan, Iran.

GRAPHICAL ABSTRACT



ARTICLE INFO

Article type:
Research Article

Article history:
Received 20 October 2023
Received in revised form 25 December 2023
Accepted 26 December 2023
Available online 28 December 2023

Keywords:
Adsorption
Methylene blue
Biochar
Kinetics
Thermodynamics



© The Author(s)
Publisher: Razi University

ABSTRACT

Agricultural product processing generates substantial quantities of agricultural waste and their disposal has become a critical concern, threatening human health and the environment. The pyrolysis process is an upgrading technology for producing valuable products from waste feedstocks. Hence, the potential of eco-friendly biochar derived from cotton waste was comprehensively investigated for methylene blue removal. The cotton-based biochar contained various pore sizes and functional groups on the surface verified by SEM and FTIR analyses. The impacts of adsorbent dose, methylene blue concentration, temperature, pH, and contact time on the adsorption of methylene blue were assessed to highlight the efficiency of the cotton-based biochar. The results revealed >90% removal under 10 mg/l methylene blue concentration, 0.7 g adsorbent dose, pH of 6, and contact time of 60 min at a temperature of 20 °C. The adsorption isotherm was well-fitted with the Freundlich model, indicating the multilayer methylene blue adsorption. The adsorption process was chemisorption and endothermic based on kinetic and thermodynamic modeling. Summing up, it can be suggested that the cotton-based biochar can be easily and efficiently applied for methylene blue removal from aqueous solutions, and further investigations are required to modify its specific surface area by a green synthesis approach.

1. Introduction

The increasing development of the textile industry in developing countries has induced the significant discharge of wastewater containing high concentrations of dyes (Putranto *et al.*, 2022). Dyes are the main contributors to environmental pollution and 15% of the dyes are highly toxic, originating from industrial activities (Bayahia, 2022; Francoeur *et al.*, 2022; Putranto *et al.*, 2022). Regarding the inorganic and organic dyes, the organic ones contain aromatic rings, leading the serious damage to water bodies (Ramutshatsha-Makhwedzha *et al.*, 2022; Francoeur *et al.*, 2022). Moreover, dye wastewater can endanger aquatic life through photosynthesis disruption, bioaccumulation, and dysfunction of ecosystems (Awais *et al.*, 2020; Ramutshatsha-Makhwedzha *et al.*, 2022). Methylene blue, as a cationic dye, is widely used in the textile, hair dye, paper, photography, and leather industries

*Corresponding author Email: hassanrezaei@gau.ac.ir

(Ramutshatsha-Makhwedzha *et al.*, 2022). Methylene blue is non-biodegradable with high toxicity, intensifying skin sensitivity, asthma, high blood pressure, and cardiovascular damage (Alshekhli *et al.*, 2020; Francoeur *et al.*, 2022). Therefore, the implementation of an efficient method for dye wastewater treatment is a priority to achieve a risk-free level and maintain environmental sustainability.

Several technologies have been employed for dye removal including membrane filtration, ion exchange, coagulation, oxidation, ozonation, and activated sludge, which have their own drawbacks (Francoeur *et al.*, 2022; Ofgea, Tura, and Fanta, 2022; Putranto *et al.*, 2022). The challenge of membrane techniques is the clogging of pores by dye molecules and the need for high filtration pressure, not only reducing the membrane efficiency and lifetime but also increasing the electricity costs (Huang *et al.*, 2017). Biological methods have high performance and guarantee the reduction of pollutants concentration in

wastewater, but the possibility of biomass accumulation, sensitivity to operational parameters such as pH and temperature, inefficient breakdown of dyes, and low flexibility limit their applications (Fahad et al., 2015; Fawcett-Hirst et al., 2021; Nemcik et al., 2022). On the other hand, the use of sedimentation tanks or physical/mechanical approaches causes toxic byproducts, significant cost, and energy consumption as well as low efficiency (Fawcett-Hirst et al., 2021; Nemcik et al., 2022). Among the available technologies, the adsorption method has been given special attention due to its high potential, simplicity, compatibility, wide application, ensuring the non-production of secondary pollutants, adsorbent reusability, and less land area requirement (Francoeur et al., 2022; Ofgea, Tura, and Fanta, 2022; Misran et al., 2022). Silica gel, alumina, activated carbon, and biochar are among the most important and widely used adsorbents. Biochar attracted more attention due to its high adsorption capacity, high specific surface area, and easy preparation (Li et al., 2017; Franciski et al., 2018; Putranto et al., 2022). However, biochar synthesis using low-cost and easily accessible precursors including banana peel, wheat straw, olive kernel, coconut shell, rice husk, and sugarcane, as well as agricultural waste can minimize the adverse environmental impacts and propose a cost-effective alternative to commercial carbon (Yao et al., 2020; de Souza et al., 2022; Phonlam et al., 2023).

In recent years, agricultural waste has occupied an irreplaceable position in biochar synthesis with the aim of wastewater remediation. Approximately 25 million cotton and about 50 million cotton waste are produced annually, covering 2.5 % of the cultivation of agricultural land in the world (Zhang et al., 2021). Regarding a large volume of unused cotton waste, the optimal utilization and sustainable management of these valuable materials should be considered instead of the conventional approaches of waste discarding and burning. The conversion of cotton waste to biofuels (Xie et al., 2019), soil conditioners (Wang et al., 2018), and ethanol (Malik et al., 2020) has been already investigated. However, to the best of our knowledge, there is limited literature considering the production of biochar derived from cotton waste for dye wastewater treatment. Hence, the present study was conducted to synthesize biochar from cotton waste for methylene blue removal. The effects of parameters such as adsorbent dosage, pH, methylene blue concentration, temperature, and contact time were assessed to obtain optimal conditions for the synthesized adsorbent. Moreover, the isotherm, kinetics, and thermodynamic equations were utilized to specify the adsorption process. The results of this study can provide a certain framework regarding the intrinsic features of agricultural waste for wastewater remediation.

2. Materials and methods

2.1. Biochar synthesis

The cotton waste was collected from the cotton fields and dried in sunlight. Then, it was powdered using the lab mill, sieved, and dried at 70 °C for 24 hours. 30 g of the as-prepared powder was burned in the pyrolysis furnace (TF5/25-1250) at a temperature of 500 °C under the nitrogen gas flow with a gas pressure of 100 ml/min for one hour (Fig. 1).

2.2. Biochar characterization

Field emission scanning electron microscopy analysis (FESEM, FEI Quanta 200 ESEM) was used to determine the size and morphology of the synthesized biochar. The amount of C, O, N, H, and S was determined by an elemental analyzer (Flash EA 1112, USA). The functional groups on the biochar surface were specified using Fourier-transform infrared spectroscopy (FTIR, Thermo Nicolet Avatar 370 FTIR, USA). The Brunauer-Emmett-Teller theory (BET, BELSORP MINI II-Japan) analysis was also performed to determine the surface area of biochar.

2.3. Optimization of methylene blue removal

To achieve the highest methylene blue removal efficiency, operating variables such as biochar dose, methylene blue concentration, temperature, contact time, and pH were considered using the on-at-a-time method with 3 replicates. Methylene blue concentrations of 5, 10, 20, 50, and 100 mg/L were evaluated at an adsorbent dose of 0.7 g and pH of 6 at room temperature for one hour. After that, the impact of cotton-based biochar dose in the range of 0.2, 0.3, 0.5, 0.7, and 1 g on the methylene blue removal was investigated considering pH of 6, methylene blue concentration of 10 mg/L, and contact time of one hour at room temperature. To optimize pH, pH values of 4, 6, 8, 10, and 12 were considered under methylene blue concentration of 10 mg/L, contact time of one hour, and adsorbent dose of 0.7 g at room temperature. Afterward, the biochar capacity was evaluated at different

temperatures including 10, 15, 20, 30, and 40 °C at the fixed condition. Moreover, the role of contact time in the removal of methylene blue was assessed at 15, 30, 60, 90, and 120 min.

2.4. Adsorption isotherm, kinetic, and thermodynamic

The Langmuir isotherm was used to highlight the interaction between sorbate molecules and the adsorbent surface (Nowrouzi et al., 2017; Bahramifar and Younesi, 2018; Peer; Al-Ghouti, and Da'ana, 2020; Einollahipeer, and Okati, 2022). This model is expressed as follows:

$$\frac{C_e}{q_e} = \frac{1}{q_m} C_e + \frac{1}{q_m b} \quad (1)$$

where, q_e and q_m denote the equilibrium and maximum adsorption capacity (mg/g), respectively. b shows the Langmuir constant and C_e shows the adsorbate concentration (mg/L) in the equilibrium condition. Freundlich model assumes the uniformity of the adsorbent surface and is described as follows (Rastgar et al., 2022):

$$\ln q_e = \frac{1}{n} \ln C_e + \ln k_F \quad (2)$$

where, $1/n$ and k_F (mg/g (L/mg)^{1/n}) illustrate the exponent and Freundlich constant, respectively.

The kinetic models of pseudo-first-order and pseudo-second-order are commonly used to predict the adsorption kinetic. The linear form of the pseudo-first-order model is described in the following equation:

$$\ln(q_e - q_t) = \ln q_e - k_1 t \quad (3)$$

where, k_1 indicates the pseudo-first-order rate constant (1/min) and q_e shows the adsorption capacity at time t (mg/g).

The pseudo-second-order is calculated as follows (Rastgar et al., 2023):

$$\frac{t}{q_t} = \frac{1}{k_2 q_e^2} + \frac{1}{q_e} t \quad (4)$$

where, t is the time (min) and k_2 is the constant rate of pseudo-second-order (g/mg. min).

The adsorption thermodynamics at various temperatures (283, 288, 293, 303, and 313 K) were investigated. The entropy (ΔS), enthalpy (ΔH), and Gibbs free energy (ΔG) were assessed by the following equations (Nowrouzi, Younesi, and Bahramifar, 2017; Nowrouzi, Younesi, and Bahramifar, 2018):

$$\Delta G = -RT \ln k_c \quad (5)$$

$$\ln k_c = \frac{\Delta S}{R} - \frac{\Delta H}{RT} \quad (6)$$

where, k_c is the equilibrium constant. T shows the temperature of the aqueous solution (K), and R denotes the gas constant (8.314 J/mol K).

3. Results and discussion

3.1. Adsorbent characterization

Elemental analysis elucidated 36.65 % carbon, 4.135 % hydrogen, 0.739 % nitrogen, and 0.381 % sulfur. The morphology of the cotton-based biochar surface was investigated through SEM analysis. Fig. 2 shows micro-cavities with various pore sizes on the surface of cotton-based biochar. The surface is relatively smooth, and the combined small particles give a sponge shape (Akram et al., 2019; Zoua et al., 2020). FTIR spectra were used to determine the functional groups in cotton-based biochar. As shown in Fig. 3, a broad peak at 3126.69 cm⁻¹ is ascribed to the O-H stretching vibration (El-Reash et al., 2023). A peak at 2037.25 cm⁻¹ corresponds to C≡C stretching of the alkynes group (Smith, 2017). A strong peak at 1638.94 cm⁻¹ represents the C=C stretching of the weak alkene group. The peak at 1453.32 cm⁻¹ is attributed to the bending vibration of -CH₂- or OCH (Espina, Sanchez-Cortes, and Jurašková, 2022; Nowrouzi, Younesi, and Bahramifar, 2018). A peak at 1107.41 cm⁻¹ can be attributed to the C-O-C stretching vibration (Ferreira et al., 2021). An absorption band at 1400.59 cm⁻¹ corresponds to CH₃ bending (Inyinbor, Adekola, and Olatunji, 2016). The pore size distribution and surface area of the cotton-based biochar were determined using BET analysis (Fig. 4). The surface area and pore size of the adsorbent were 3.99 m²/g and 24.04 nm, respectively. The adsorption isotherm depicted a hysteresis loop, indicating the simultaneous micro and mesoporosity (IV type) based on the International Union of Pure and Applied Chemistry (IUPAC) classification. Zhang et al. (2021) also reported the surface area of pretreated cotton stalk hydrochars in the range of 3.75 to 22.3 m²/g. It was speculated acid/base treatment can produce complex products and block the pores.

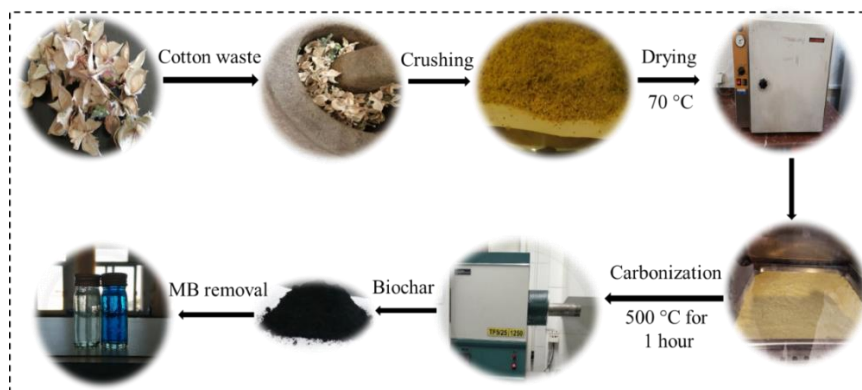


Fig. 1. Schematic diagram of biochar synthesis.

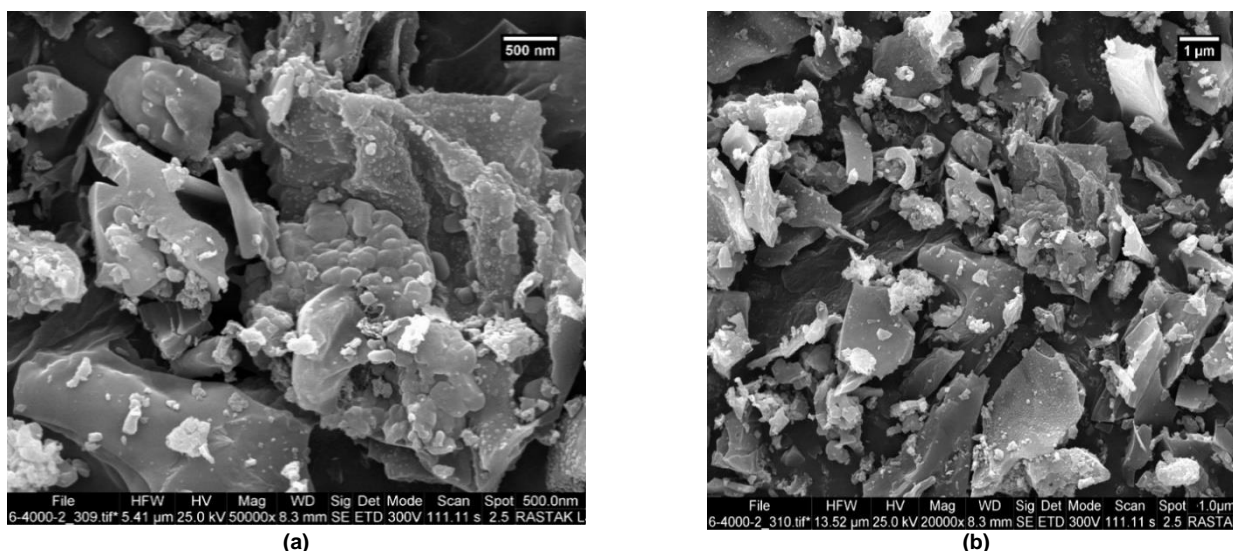


Fig. 2. SEM image of cotton-based biochar with magnification of (a) 50 kx and (b) 20 kx.

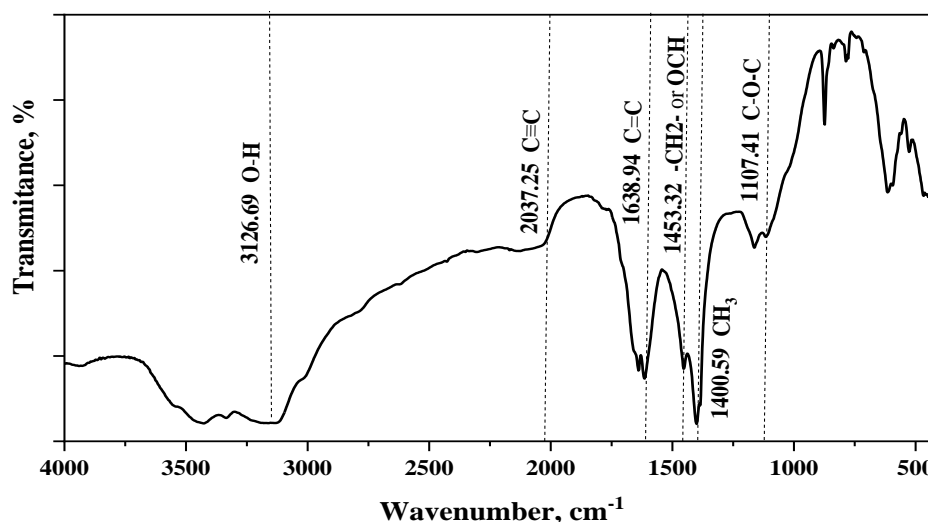


Fig. 3. FTIR spectra of cotton-based biochar.

3.2. Effect of pH

The methylene blue adsorption efficiency of the cotton-based biochar was assessed in the pH value of 4 to 12 as depicted in Fig. 5a. The increase of pH from 4 to 12 showed the enhancement of adsorption capacity from 2.97 mg/g to 3.18 mg/g. The relative fluctuations were observed in the pH of 4 to 10 and the methylene blue removal was changed in the range of 87.03% to 89.05 %. However, in terms of adsorption capacity, the maximum q_e was detected at a pH of 12 with 95.4% removal. The increasing trend of adsorption capacity in response to pH rise can be described as follows: H^+ ions at low pH compete with cationic methylene blue ions for the limited binding sites on the cotton-based biochar, hindering the adsorption of methylene blue molecules and reducing the removal efficiency (Fan *et al.*, 2017). On the other

hand, as the pH increased, the repulsive interaction between H^+ ions and methylene blue molecules reduced, increasing the adsorption capacity (Fan *et al.*, 2017). In addition, the electrostatic attraction of methylene blue by cotton-based biochar at a pH value of more than 4.8 could be related to the interactions with carboxyl and hydroxyl functional groups (Lyu *et al.*, 2018). Similar results have been reported for methylene blue removal by $ZnFe_2O_4$ nanoparticles (Zhang *et al.*, 2017), banana pseudostem biochar (Liu *et al.*, 2019), and biochars produced from rapeseed, whitewood, and seaweed (Güleç *et al.*, 2022). Zhang *et al.* (2020) investigated the potential of biochar/iron oxide composite in methylene blue adsorption and manifested the enhancement in adsorption capacity from 2.82 mg/g at pH 2.05 to 118.27 mg/g at pH 9.21, confirming the results of the current study.

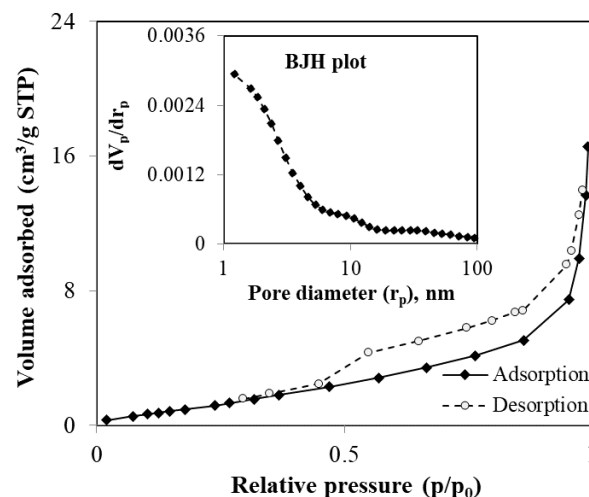


Fig. 4. Adsorption and desorption isotherm of cotton-based biochar and pore size distribution using BJH plot.

3.3. Effect of biochar dose

Fig. 5b reveals the decreasing trend in the adsorption capacity of cotton-based biochar from 4.1 mg/g to 0.98 mg/g as the adsorbent dose altered in the range of 0.2 g to 1 g. The maximum removal of methylene blue was detected at an adsorbent dose of 1 g equal to 97.87%. This finding can be associated with an increase in available active sites for methylene blue molecules (Zhang *et al.*, 2020). However, the adsorption capacity decreased with the biochar dose increase, which can be related to a relative decrease in the active adsorption sites or the number of methylene blue molecules per unit of adsorbent (Santhosh *et al.*, 2017; Zhang *et al.*, 2020). Fan *et al.* (2017) also evaluated the removal of methylene blue using sludge-derived biochar and reported a 98% removal efficiency when the biochar dose increased from 6 to 8 g/L.

3.4. Effect of methylene blue concentration

The effect of methylene blue concentration on adsorption efficiency is demonstrated in Fig. 5c. As shown, the adsorption capacity enhanced from 0.68 mg/g to 10.18 mg/g while the methylene blue concentration increased in the range of 5 to 100 mg/L, which could be ascribed to a driving force of mass transfer and increase of interaction between dye molecules with adsorption sites (Güleç *et al.*, 2022). In other words, the driving force was raised in parallel to an increase in dye concentration that overcame the mass transfer resistance and enhanced the adsorption capacity (Pandey *et al.*, 2022; Su *et al.*, 2022). In addition, the highest percentage of methylene blue removal (95.86%) was estimated at 10 mg/L methylene blue concentration, which declined to 71.25% at 100 mg/L methylene blue concentration. It should be mentioned that at low dye concentrations, more adsorption sites are available for dye molecules to adsorb on the biochar surface, raising the removal efficiency (Gao *et al.*, 2022). In contrast, the active accessible sites were gradually occupied by sorbate molecules with the dye concentration increment, leading to a decline in the removal potential of biochar (Einollahipeer and Okati, 2022). Liu, Li and Singh (2021) assessed the potential of biochar prepared from lignin and modified with manganese in adsorbing methylene blue and declared that the adsorption rate of methylene blue was higher at low dye concentrations (98.6%). Regarding the obtained results, the methylene blue removal at the concentration of 20 mg/L was more than 94%.

3.5. Effect of contact time

The effect of contact time on the methylene blue adsorption is illustrated in Fig. 5d. An increase in contact time from 15 to 120 min led to a low increment of about 5% in the removal potential. However, the adsorption capacity of cotton-based biochar was relatively constant in all considered contact times (2.55 mg/g), indicating that the adsorption capability of biochar was independent of contact time. The most methylene blue removal (87.79%) was achieved at the initial 15 min due to more vaccine-available active sites (Rastgar *et al.*, 2022). Suhaimi *et al.* (2022) declared the highest methylene blue removal (~80%) at an

initial 40 min. Another literature (Rastgar *et al.*, 2022) showed an increase in dye removal from 22.63% to 74.7% with an increase in contact time to 120 min. Fan *et al.* (2017) achieved the proper contact time of methylene blue removal in the range of 8 to 10 hours.

3.6. Effect of temperature

The methylene blue adsorption efficiency of cotton-based biochar indicated the optimal temperature at 20 °C (Fig. 5e). Notably, the change of temperature from 10 °C to 40 °C depicted an insignificant difference between the adsorption capacity values (2.39-2.75 mg/g). Furthermore, the highest and lowest dye removals were attained at the temperatures of 10 °C (84.38%) and 20 °C (96.46%), respectively. Güleç *et al.* (2022) appraised the methylene blue removal through different thermal conversion technologies. The biochar produced from brown seaweed (*Laminaria Digitata*) indicated the maximum dye uptake rate equivalent to 160 mg/g at 30 °C and 40 °C and also highlighted that the dye uptake is not directly attributed to adsorbent surface area or pore volume. Additionally, when the temperature is increased, the interaction forces between the solvent and solute molecules become weaker and the solute is easily adsorbed on the adsorbent (Ganesan, Kamaraj, and Vasudevan, 2013). The biochar capability for methylene blue removal was also compared with other adsorbents as depicted in Table 1. Notably, the cotton-based biochar could maintain 80% of its capacity for methylene blue removal after 20 cycles.

3.7. Adsorption isotherms, kinetics, and thermodynamics

According to Fig. 6, the empirical data was well-fitted with the Freundlich model (0.9596) as shown in Table 2. It demonstrated that the adsorption was carried out in multi-layers on the heterogeneous surface and uneven distribution of energy. The value of $1/n$ in the Freundlich equation indicates the adsorption intensity of the methylene blue molecules on the adsorbent and was estimated as 0.49, demonstrating a favorable adsorption isotherm (Shen *et al.*, 2015; Weng *et al.*, 2023). In terms of kinetic study (Fig. 7), the pseudo-second-order model (0.999) confirmed the adsorption as a chemisorption process, which displayed the involvement of valence force between methylene blue molecules and adsorbent through electron exchange (Ramutshatsha-Makhwedzha *et al.*, 2022). The negative and greater values of ΔG manifested spontaneity and a more vigorous adsorption process, respectively (Nowrouzi, Younesi, and Bahramifar, 2018). According to Table 2, the negative value of ΔG° enhanced with the temperature increase, implying the increase of methylene blue adsorption on cotton-based biochar (Durrani *et al.*, 2022). The positive value of ΔS elucidated the randomness and irreversible adsorption process. Moreover, the positive ΔH value elucidated that the methylene blue adsorption is endothermic. Similar results have been reported in previous investigations (Rashid *et al.*, 2016; Yağmur and Kaya, 2021; Durrani *et al.*, 2022).

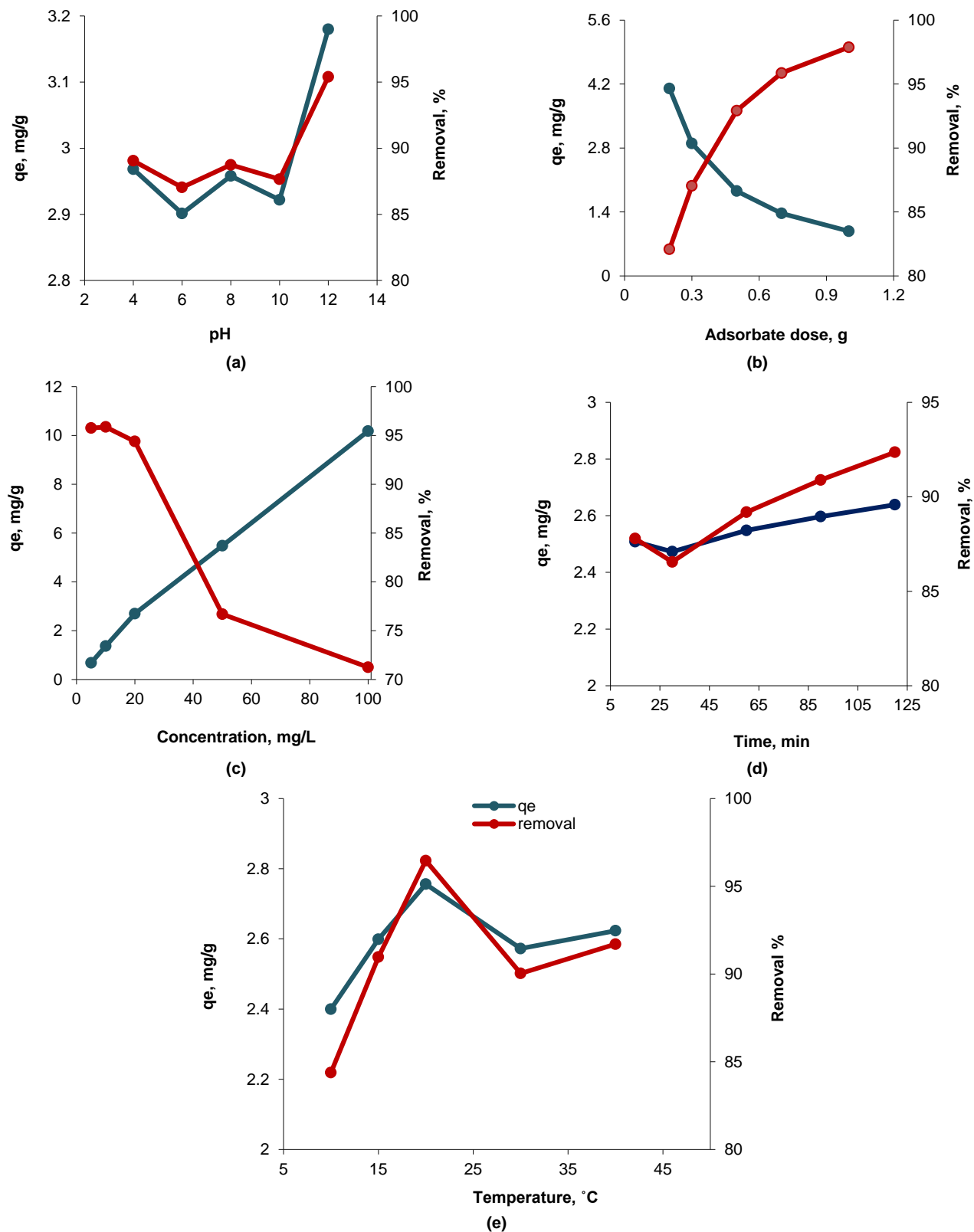
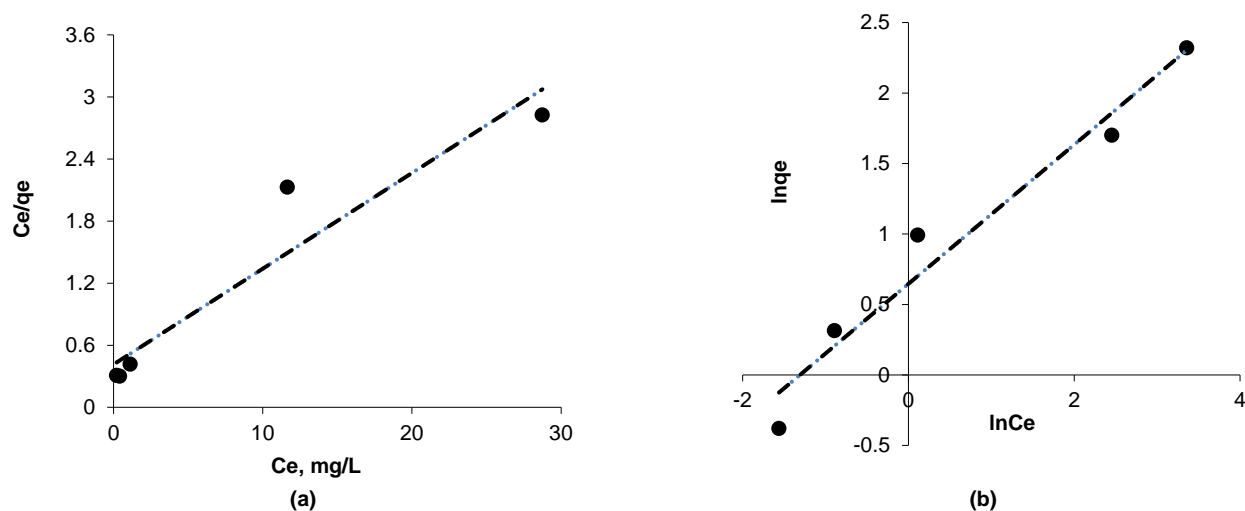
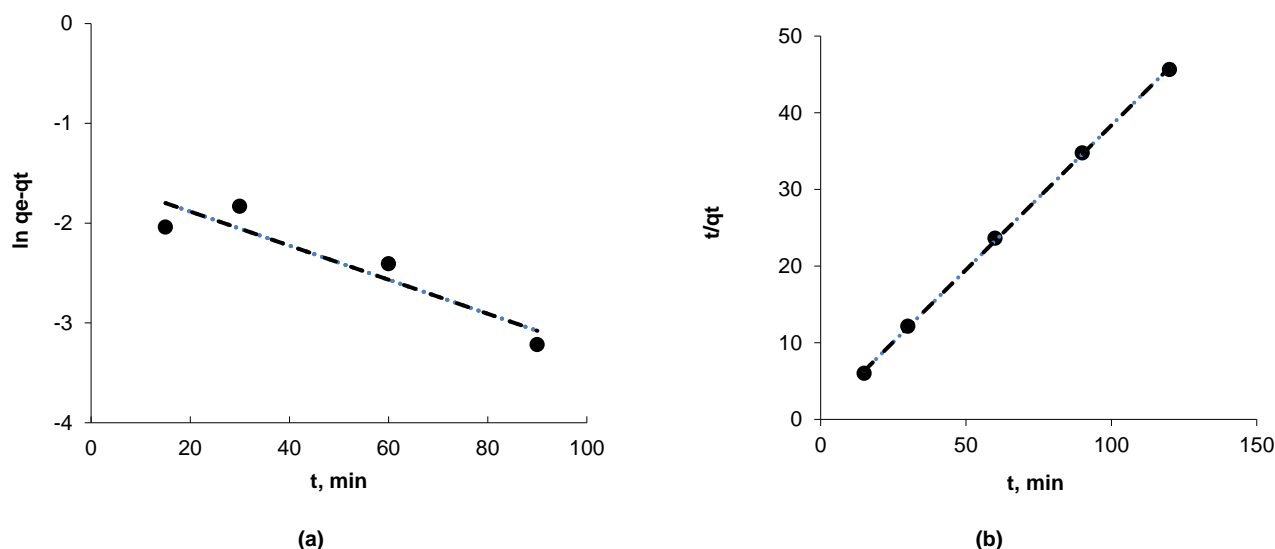


Fig. 5. The impacts of operational parameters on the adsorption capacity of cotton-based biochar, (a) pH, (b) Adsorbent dose, (c) methylene blue concentration, (d) contact time, (e) and temperature.

Table 1. Comparison of biosorbent potential for methylene blue removal.

Adsorbent	Methylene blue Concentration, mg/l	Contact time, min	Adsorbent dose, g	Removal, %	Adsorption capacity, mg/g	Ref.
Cotton-based biochar	10	60	0.7	>90	10.81	This study
CS-H ₂ SO ₄ +NaOH-HTC	50	120	0.07	100	198	(Zhang et al., 2021)
Cotton-stalk activated carbon fibers (CSCFs)	5	240	-	97	-	(Li et al., 2017)
<i>Eucheuma cottonii</i> seaweed biochar	200	360	-	-	133.3	(Saeed et al., 2020)
Wheat straw biochar	100	300	0.06	-	12.03	(Liu et al., 2012)

**Fig. 6.** (a) Langmuir, and (b) Freundlich isotherm models for methylene blue adsorption.**Fig. 7.** (a) Pseudo-first-order, and (b) pseudo-second-order models for methylene blue removal.

4. Conclusions

This study was conducted to provide a cost-effective and high-efficiency biochar derived from cotton waste for methylene blue removal. The results of this investigation present an approach not only for cotton waste disposal but also for dye wastewater treatment. The optimal condition to achieve the maximum methylene blue removal was a pH of 6, 0.7 g adsorbent dose, 10 mg/l methylene blue concentration, and 1

hour contact time at 20 °C. The experimental data was well fitted with the Freundlich isotherm model, showing desirable and multilayer adsorption. Moreover, the adsorption process was endothermic and spontaneous based on the thermodynamic study. According to the acceptable removal of methylene blue (>90%) using cotton-based biochar without chemical activation, it can be recommended as an affordable and available adsorbent for industrial wastewater treatment.

Table 2. Kinetic and isotherm parameters for methylene blue adsorption by cotton-based biochar

Isotherms	Parameters	Value
Langmuir	q_m , mg/g	10.81
	B , L/mg	0.22
	R^2	0.9099
Freundlich	K_F , (mg/g)/(mg/L) ⁿ	1.908
	1/n	0.4938
	R^2	0.9596
Kinetics		
Pseudo-first order	q_e , mg/g	4.677
	K_1 , min ⁻¹	0.0171
	R^2	0.8638
Pseudo-second order	q_e , mg/g	2.65
	K_2 , g/mg min	0.2017
	R^2	0.9997
Thermodynamics		
Temperature, K	ΔG , kJ/mol	ΔH , kJ/mol
283	742.41	8493.58
288	-951.47	ΔS (kJ/mol K)
293	-3290.23	32.277
303	-596.23	
313	-1186.71	

Author Contributions

Samaneh Salmani: Conceptualization, investigation, methodology, and writing- original draft.

Hassan Rezaei: Supervision, validation, review, and editing.

Hajar Abyar: Investigation, methodology, analysis, review, and editing.

Conflict of Interest

The authors declare that they have no known competing financial interests or personal relationships that could have appeared to influence the work reported in this paper.

Acknowledgments

The authors would like to thank Gorgan University of Agricultural Sciences and Natural Resources, Iran, for their support.

Data Availability Statement

The datasets used in the current study are available on request.

References

- Akram, M. *et al.* (2019) 'Biosorption of lead by cotton shells powder: characterization and equilibrium modeling study', *International journal of phytoremediation*, 21, pp. 138-144. doi: <https://doi.org/10.1080/15226514.2018.1488810>
- Al-Ghouti, M. A., and Da'ana, D. A. (2020) 'Guidelines for the use and interpretation of adsorption isotherm models: A review', *Journal of hazardous materials*, 393, pp. 122383. doi: <https://doi.org/10.1016/j.jhazmat.2020.122383>
- Alshekhli, A. F. *et al.* (2020) 'Development of adsorbent from phytoremediation plant waste for methylene blue removal', *Journal of Ecological Engineering*, 21, pp. 207-215. doi: <https://doi.org/10.12911/22998993/126873>
- Awais, A. *et al.* (2020) 'A novel study on synthesis of egg shell based activated carbon for degradation of methylene blue via photocatalysis', *Arabian Journal of Chemistry*, 13, pp. 8717-8722. doi: <https://doi.org/10.1016/j.arabjc.2020.10.002>
- Bayahia, H. (2022) 'Green synthesis of activated carbon doped tungsten trioxide photocatalysts using leaf of basil (*Ocimum basilicum*) for photocatalytic degradation of methylene blue under sunlight', *Journal of Saudi Chemical Society*, 26, pp. 101432. doi: <https://doi.org/10.1016/j.jscs.2022.101432>
- de Souza, C. C. *et al.* (2022) 'Activated carbon of *Coriandrum sativum* for adsorption of methylene blue: Equilibrium and kinetic modeling', *Cleaner Materials*, 3, pp. 100052. doi: <https://doi.org/10.1016/j.clema.2022.100052>
- Durrani, W. Z. *et al.* (2022) 'Adsorption efficiency of date palm based activated carbon-alginate membrane for methylene blue', *Chemosphere*, 302, pp. 134793. doi: <https://doi.org/10.1016/j.chemosphere.2022.134793>
- Einollahipeer, F., and Okati, N. (2022) 'High efficient Hg (II) and TNP removal by NH₂ grafted magnetic graphene oxide synthesized from *Typha latifolia*', *Environmental Technology*, 43, pp. 3956-3972. doi: <https://doi.org/10.1080/09593330.2021.1937708>
- El-Reash, Y. A. *et al.* (2023) 'Highly fluorescent hydroxyl groups functionalized graphitic carbon nitride for ultrasensitive and selective determination of mercury ions in water and fish samples', *Journal of Analytical Science and Technology*, 14, pp. 16. doi: <https://doi.org/10.1186/s40543-023-00379-0>
- Espina, A., Sanchez-Cortes, S., and Jurašková, Z. (2022) 'Vibrational study (Raman, SERS, and IR) of plant gallnut polyphenols related to the fabrication of iron gall inks', *Molecules*, 27, pp. 279. doi: <https://doi.org/10.3390/molecules27010279>
- Fahad, A. *et al.* (2015) 'Wastewater and its Treatment Techniques: An Ample', *Indian Journal of Science and Technology*, 12, pp. 25. doi: <https://doi.org/10.17485/ijst/2019/v12i25/146059>
- Fan, S. *et al.* (2017) 'Removal of methylene blue from aqueous solution by sewage sludge-derived biochar: Adsorption kinetics, equilibrium, thermodynamics and mechanism', *Journal of Environmental Chemical Engineering*, 5, pp. 601-611. doi: <https://doi.org/10.1016/j.jece.2016.12.019>
- Fawcett-Hirst, W. *et al.* (2021) 'A review of treatment methods for insensitive high explosive contaminated wastewater', *Heliyon*, 7. doi: <https://doi.org/10.1016/j.heliyon.2021.e07438>
- Ferreira, N. S. *et al.* (2021) 'Visible-light-responsive photocatalytic activity significantly enhanced by active [V_{2n}+ V₀]⁺ defects in self-assembled ZnO nanoparticles', *Inorganic Chemistry*, 60, pp. 4475-4496. doi: <https://doi.org/10.1021/acs.inorgchem.0c03327>
- Franciski, M. A. *et al.* (2018) 'Development of CO₂ activated biochar from solid wastes of a beer industry and its application for methylene blue adsorption', *Waste Management*, 78, pp. 630-638. doi: <https://doi.org/10.1016/j.wasman.2018.06.040>
- Francoeur, M. *et al.* (2022) 'Optimization of the synthesis of activated carbon prepared from *Sargassum* (sp.) and its use for tetracycline, penicillin, caffeine and methylene blue adsorption from contaminated water', *Environmental Technology & Innovation*, 28, pp. 102940. doi: <https://doi.org/10.1016/j.eti.2022.102940>
- Ganesan, P., Kamaraj, R., and Vasudevan, S. (2013) 'Application of isotherm, kinetic and thermodynamic models for the adsorption of nitrate ions on graphene from aqueous solution', *Journal of the Taiwan Institute of Chemical Engineers*, 44, pp. 808-814. doi: <https://doi.org/10.1016/j.jtice.2013.01.029>
- Gao, Y. *et al.* (2022) 'Steam activation tuned porous structure and surface wetting behaviors of mesoporous biochars for corrosive oily wastewater treatments', *Journal of Chemical Technology & Biotechnology*, 97, pp. 2179-2185. doi: <https://doi.org/10.1002/jctb.7096>
- Güleç, F. *et al.* (2022) 'A comprehensive comparative study on methylene blue removal from aqueous solution using biochars produced from rapeseed, whitewood, and seaweed via different

- thermal conversion technologies', *Fuel*, 330, pp. 125428. doi: <https://doi.org/10.1016/j.fuel.2022.125428>
- Huang, Z. et al. (2017) 'Modified bentonite adsorption of organic pollutants of dye wastewater', *Materials Chemistry and Physics*, 202, pp. 266-276. doi: <https://doi.org/10.1016/j.matchemphys.2017.09.028>
- Inyinbor, A., Adekola, F., and Olatunji, G. A. (2016) 'Kinetics, isotherms and thermodynamic modeling of liquid phase adsorption of Rhodamine B dye onto *Raphia hookerie* fruit epicarp', *Water Resources and Industry*, 15, pp. 14-27. doi: <https://doi.org/10.1016/j.wri.2016.06.001>
- Li, K. et al. (2017) 'Preparation of nitrogen-doped cotton stalk microporous activated carbon fiber electrodes with different surface area from hexamethylenetetramine-modified cotton stalk for electrochemical degradation of methylene blue', *Results in physics*, 7, pp. 656-664. doi: <https://doi.org/10.1016/j.rinp.2017.01.030>
- Liu, S. et al. (2019) 'A modified method for enhancing adsorption capability of banana pseudostem biochar towards methylene blue at low temperature', *Bioresource technology*, 282, pp. 48-55. doi: <https://doi.org/10.1016/j.biortech.2019.02.092>
- Liu, X.-J., Li, M.-F., and Singh, S. K. (2021) 'Manganese-modified lignin biochar as adsorbent for removal of methylene blue', *Journal of materials research and technology*, 12, pp. 1434-1445. doi: <https://doi.org/10.1016/j.jmrt.2021.03.076>
- Liu, Y. et al. (2012) 'Characterization of bio-char from pyrolysis of wheat straw and its evaluation on methylene blue adsorption', *Desalination and Water Treatment*, 46, pp. 115-123. doi: <https://doi.org/10.1080/19443994.2012.677408>
- Lyu, H. et al. (2018) 'Experimental and modeling investigations of ball-milled biochar for the removal of aqueous methylene blue', *Chemical Engineering Journal*, 335, pp. 110-119. doi: <https://doi.org/10.1016/j.cej.2017.10.130>
- Malik, K. et al. (2020) 'Enhanced ethanol production by *Saccharomyces cerevisiae* fermentation post acidic and alkali chemical pretreatments of cotton stalk lignocellulose', *International Biodeterioration & Biodegradation*, 147, pp. 104869. doi: <https://doi.org/10.1016/j.ibid.2019.104869>
- Misran, E. et al. (2022) 'Banana stem based activated carbon as a low-cost adsorbent for methylene blue removal: Isotherm, kinetics, and reusability', *Alexandria Engineering Journal*, 61, pp. 1946-1955. doi: <https://doi.org/10.1016/j.aej.2021.07.022>
- Nemcik, J. et al. (2022) 'Wastewater Treatment Modeling Methods Review', *IFAC-PapersOnLine*, 55, pp. 195-200. doi: <https://doi.org/10.1016/j.ifacol.2022.06.032>
- Nowrouzi, M. et al. (2017) 'An enhanced counter-current approach towards activated carbon from waste tissue with zero liquid discharge', *Chemical Engineering Journal*, 326, pp. 934-944. doi: <https://doi.org/10.1016/j.cej.2017.05.141>
- Nowrouzi, M., Younesi, H., and Bahramifar, N. (2017) 'High efficient carbon dioxide capture onto as-synthesized activated carbon by chemical activation of Persian Ironwood biomass and the economic pre-feasibility study for scale-up', *Journal of Cleaner Production*, 168, pp. 499-509. doi: <https://doi.org/10.1016/j.jclepro.2017.09.080>
- Nowrouzi, M., Younesi, H., and Bahramifar, N. (2018) 'Superior CO₂ capture performance on biomass-derived carbon/metal oxides nanocomposites from Persian ironwood by H₃PO₄ activation', *Fuel*, 223, pp. 99-114. doi: <https://doi.org/10.1016/j.fuel.2018.03.035>
- Ofgea, N. M., Tura, A. M., and Fanta, G. M. (2022) 'Activated carbon from H₃PO₄-activated *Moringa stenopetale* seed husk for removal of methylene blue: optimization using the response surface method (RSM)', *Environmental and Sustainability Indicators*, 16, pp. 100214. doi: <https://doi.org/10.1016/j.indic.2022.100214>
- Pandey, D. et al. (2022) 'Valorization of waste pine needle biomass into biosorbents for the removal of methylene blue dye from water: Kinetics, equilibrium and thermodynamics study', *Environmental Technology & Innovation*, 25, pp. 102200. doi: <https://doi.org/10.1016/j.eti.2021.102200>
- Peer, F. E., Bahramifar, N., and Younesi, H. (2018) 'Removal of Cd (II), Pb (II) and Cu (II) ions from aqueous solution by polyamidoamine dendrimer grafted magnetic graphene oxide nanosheets', *Journal of the Taiwan Institute of Chemical Engineers*, 87, pp. 225-240. doi: <https://doi.org/10.1016/j.jtice.2018.03.039>
- Phonlam, T. et al. (2023) 'Ammonia modification of activated carbon derived from biomass via gamma irradiation vs. hydrothermal method for methylene blue removal', *South African Journal of Chemical Engineering*, 43, pp. 67-78. doi: <https://doi.org/10.1016/j.sajce.2022.10.004>
- Putranto, A. et al. (2022) 'Effects of pyrolysis temperature and impregnation ratio on adsorption kinetics and isotherm of methylene blue on corn cobs activated carbons', *South African Journal of Chemical Engineering*, 42, pp. 91-97. doi: <https://doi.org/10.1016/j.sajce.2022.07.00>
- Ramutshatsha-Makhwedzha, D. et al. (2022) 'Activated carbon derived from waste orange and lemon peels for the adsorption of methyl orange and methylene blue dyes from wastewater', *Heliyon*, 8. doi: <https://doi.org/10.1016/j.heliyon.2022.e09930>
- Rashid, R. A. et al. (2016) 'KOH-activated carbon developed from biomass waste: adsorption equilibrium, kinetic and thermodynamic studies for Methylene blue uptake', *Desalination and Water Treatment*, 57, pp. 27226-27236. doi: <https://doi.org/10.1080/19443994.2016.1167630>
- Rastgar, S. et al. (2022) 'Low-cost magnetic char derived from oily sludge for Methylene Blue dye removal: optimization, isotherm, and kinetic approach', *Advances in Environmental Technology*, 8, pp. 329-343. doi: <https://doi.org/10.22104/AET.2022.5795.1595>
- Rastgar, S. et al. (2023) 'Photocatalytic degradation of methylene blue (MB) dye under UV light irradiation by magnetic diesel tank sludge (MDTS)', *Biomass Conversion and Biorefinery*, pp. 1-12. doi: <https://doi.org/10.1007/s13399-023-04062-7>
- Saeed, A. A. H. et al. (2020) 'Eucheuma cottonii seaweed-based biochar for adsorption of methylene blue dye', *Sustainability*, 12, pp. 10318. doi: <https://doi.org/10.3390/su122410318>
- Santhosh, C. et al. (2017) 'Magnetic SiO₂@CoFe₂O₄ nanoparticles decorated on graphene oxide as efficient adsorbents for the removal of anionic pollutants from water', *Chemical Engineering Journal*, 322, pp. 472-487. doi: <https://doi.org/10.1016/j.cej.2017.03.144>
- Shen, X. et al. (2015) 'Sorption mechanisms of organic compounds by carbonaceous materials: site energy distribution consideration', *Environmental Science & Technology*, 49, pp. 4894-4902. doi: <https://doi.org/10.1021/es506034e>
- Smith, B. C. (2017) 'An IR spectral interpretation potpourri: carbohydrates and alkynes', *Spectroscopy*, 32, pp. 18-24. Available at: <https://www.spectroscopyonline.com/view/ir-spectral-interpretation-potpourri-carbohydrates-and-alkynes> (Accessed: 1 July 2017).
- Su, H. et al. (2022) 'Ultrafine biosorbent from waste oyster shell: A comparative study of Congo red and Methylene blue adsorption', *Bioresource technology reports*, 19, pp. 101124. doi: <https://doi.org/10.1016/j.biteb.2022.101124>
- Suhaimi, N. et al. (2022) 'The use of *Gigantochloa* bamboo-derived biochar for the removal of methylene blue from aqueous solution', *Adsorption Science & Technology*, 2022, pp. 1-12. doi: <https://doi.org/10.1155/2022/8245797>
- Wang, Z. et al. (2018) 'Characteristics of biochars prepared by co-pyrolysis of sewage sludge and cotton stalk intended for use as soil amendments', *Environmental Technology*. doi: <https://doi.org/10.1080/09593330.2018.1534891>
- Weng, T. et al. (2023) 'The effect of micro-and nano-γ-Al₂O₃ on the synthetic hydrotalcite and Congo red adsorption: Site energy distribution', *Journal of Molecular Liquids*, 388, pp. 122708. doi: <https://doi.org/10.1016/j.molliq.2023.122708>
- Xie, Y. et al. (2019) 'Solar pyrolysis of cotton stalk in molten salt for bio-fuel production', *Energy*, 179, pp. 1124-1132. doi: <https://doi.org/10.1016/j.energy.2019.05.055>
- Yağmur, H. K., and Kaya, İ. (2021) 'Synthesis and characterization of magnetic ZnCl₂-activated carbon produced from coconut shell for the adsorption of methylene blue', *Journal of molecular structure*, 1232, pp. 130071. doi: <https://doi.org/10.1016/j.molstruc.2021.130071>
- Yao, X. et al. (2020) 'Magnetic activated biochar nanocomposites derived from wakame and its application in methylene blue adsorption', *Bioresource technology*, 302, pp. 122842. doi: <https://doi.org/10.1016/j.biortech.2020.122842>
- Zhang, L. et al. (2021) 'Cotton stalk-derived hydrothermal carbon for methylene blue dye removal: Investigation of the raw material plant

- tissues', *Bioresources and Bioprocessing*, 8, pp. 1-11. doi: <https://doi.org/10.1186/s40643-021-00364-8>
- Zhang, P. et al. (2017) 'High efficiency removal of methylene blue using SDS surface-modified ZnFe₂O₄ nanoparticles', *Journal of Colloid and Interface Science*, 508, pp. 39-48. doi: <https://doi.org/10.1016/j.jcis.2017.08.025>
- Zhang, P. et al. (2020) 'A green biochar/iron oxide composite for methylene blue removal', *Journal of hazardous materials*, 384, pp. 121286. doi: <https://doi.org/10.1016/j.jhazmat.2019.121286>
- Zoua, Y. et al. (2020) 'Pb²⁺ removal performance by cotton-based and magnetic modified cotton-based biochar prepared from agricultural waste biomass', *Desalination and Water Treatment*, 207, pp. 246-257. doi: <https://doi.org/10.5004/dwt.2020.26425>